Int.J.Curr.Microbiol.App.Sci (2022) *11*(02): 67-87

International Journal of Current Microbiology and Applied Sciences
ISSN: 2319-7706 **Volume 11 Number 02 (2022)**
Journal homepage: http://www.ijcmas.com

Original Research Article https://doi.org/10.20546/ijcmas.2022.1102.010

Pathological Characterization of the Low Doses Alloxan-STZ Diabetic Rabbit Model

Masood Saleem Mir[1*], Reashma Roshan[2], Omer Khalil Baba[1], Majid Shafi[1], Showkeen Muzamil Bashir[3] and Imtiyaz Wani[4]

[1]Department of Veterinary Pathology, Faculty of Veterinary Sciences & Animal Husbandry, SKUAST-Kashmir, Alusteng, Shuhama 190006, J&K, India
[2]Department of Hematology, Sher-i-Kashmir Institute of Medical Sciences (SKIMS), Soura Srinagar 190011, J&K, India
[3]Department of Veterinary Biochemistry, Faculty of Veterinary Sciences & Animal Husbandry, SKUAST-Kashmir, Alusteng, Shuhama 190006, J&K, India
[4]Department of Clinical Research, Sher-i-Kashmir Institute of Medical Sciences (SKIMS), Soura Srinagar 190011, J&K, India

**Corresponding author*

Keywords

Hyperglycemia, pathogenesis, immunity, hypoglycaemic drugs

Article Info

Received:
05 January 2022
Accepted:
30 January 2022
Available Online:
10 February 2022

A B S T R A C T

Purpose: Present investigation was aimed at characterization of pathomorphological lesions in the Low Doses Alloxan-STZ Diabetic Rabbit Model. Method: New Zealand White rabbits, 1-1.5 kg body weight, were administered alloxan (@50mg/kg b.w) and STZ (@35mg/kg b.w) cocktail, as single intravenous dose followed by glucose therapy after 9 hours. Blood glucose was regularly monitored and with blood glucose >200mg/dl on day 7 following drug administration were used for study. Two rabbits each were sacrificed fortnightly from days 15 to 60 for pathoanatomical investigation. Results: Gross lesions included congestion, and haemorrhages in different organs. Histopathologically, pancreas revealed variable degeneration and loss of beta-cells in the islets; and acinar cell degeneration. Changes were milder at later stages. Liver revealed vascular congestion, progressive hepatosis, portal triaditis, and presence of binucleated hepatocytes. During later stage hepatocellular necrosis was seen. Kidneys revealed vascular congestion; focal haemorrhages; cortical tubular degeneration and necrosis; lower nephron nephrosis; glomerular congestion and hypersegmentation; mesangial cell hyperplasia and focal nephritis with mononuclear cell infiltration. Later, peritubular fibroplasias; glomerular hypertrophy with vacuolation of podocytes and fragmentation; and casts in collecting tubules were seen. Brain revealed neuronal degeneration and necrosis in cerebral cortex, caudoputamen, different areas of hippocampus including dentate gyrus and *Cornu Ammonis* especially pyramidal cells of CA4 region, subiculum and brain stem; demyelination and gliosis in medullary tracts; mild purkinje cell degeneration and karyorrhexis in cells of granule layer; choroid epithelial degeneration; and vascular congestion. Lungs revealed vascular congestion, haemorrhages, emphysema, atelectasis, peribronchial lymphoid hyperplasia, focal pneumonia, hypertrophy of vascular walls, vacuolation of pneumocytes and presence of numerous alveolar macrophages. Heart showed vascular congestion, focal haemorrhages and degeneration of cardiomyocytes. Spleen revealed congestion, haemorrhage, apoptosis of lymphoid cells, and vacuolation of reticular cells. histiocytic reaction was additionally noted in MLNs. Congestion, degeneration and necrosis were seen in zona glomerulosa and zona fasciculate of adrenal-cortex and also, in adrenal-medulla. Changes in testes were characteristic of arrested spermatogenesis, and degeneration and apoptosis of spermatocytes. Conclusion: It could be concluded that the progressive and marked pathomorphological alterations suggest Alloxan-STZ diabetic rabbits shall be a good short term model for diabetes associated investigation when weighed appropriately against internal control.

Introduction

Diabetes mellitus is characterized by persistent hyperglycemia either due to relative or absolute lack of insulin (Type-1) or insulin resistance (Type-2). In both cases, hyperglycemia has wide spread pathological implication compromising immunity, reparative mechanisms as well as causing multiple organopathies due to reactive oxygen species. Higher global prevalence of the disease and the burden of its associated complication in the patients instigate the researchers for investigation into the disease for understanding its pathogenesis, implications under varying epidemiological conditions and screening of pharmaceuticals for preventive and therapeutic use (Ettaro *et al.,* 2004; Srinivasan and Ramarao, 2007; Etuk, 2010; King, 2012).

Studies in animal models constitute an important source of information vis-à-vis diabetes, its complications as well as effect of hypoglycaemic drugs. Chemically induced models are routinely used for such studies. The most commonly used chemicals are alloxan and sttreptozotocin, both of which induce hyperglycemia by causing selective destruction of beta cells in pancreatic islets leading to insulin deficiency (Kottaisamy *et al.,* 2021). Such models have been found appropriate for screening of non-beta-cell-dependent hypoglycaemia agents, and management of diabetic complications. However, the models need to be critically weighed for spontaneous recovery and direct toxic implications for the drugs. While spontaneous recovery following short period of hyperglycemia has been observed in low dose models, higher doses have been associated with damage to different organs. The choice of beta-cytotoxic drug used also depends upon species, strains and sex of the animal due to their varying degrees of sensitivity (Mir *et al.,* 2015). Further, batch differences in the activity warrant use of internal controls for characterization of models (Srinivasan and Ramarao, 2007; Kramer *et al.,* 2009; Grossman *et al.,* 2010). In order to minimize the direct toxic effects of the beta-cytotoxins, and produce hyperglycemia over a desired period of time, low dose drug combinations models have been developed (Mir *et al.,* 2016).

The choice of a model for a given study is critical in order to provide logical interpretation and conclusion (Thatte, 2009). Besides successfully achieving hyperglycemia over the requisite study period, a model warrants characterization for development and progression of diabetic complication (Noshahr *et al.,* 2020). Present investigation was aimed at characterization pathological alterations in low doses alloxan-STZ diabetic rabbit model.

Materials and Methods

Experimental Animals

New Zealand white rabbits of three months age and weighing about 1 to 1.5 kg were utilized in the study. the rabbits were procured from Laboratory Animal Resource and maintained under standard conditions in cage system, offering feed and water *ad libtum.* Feed and greens were offered in morning and evening. The Institutional Animal Ethics Committee approved the experimental protocols involved in this study. Following a period of 7 days acclimatization, the rabbits were allocated to control and experimental groups.

Development of Diabetic Model

Alloxan monohydrate and streptozotocin were procured from Sigma-Aldrich. Freshly prepared solutions of calculated doses were given to experimental rabbits as a cocktail. The rabbits were fasted for 18 hours prior to drug administration. Their fasting blood glucose level was noted using Accu-Chek, glucometer (Roche diagnostics India Pvt. Ltd., Mumbai). Alloxan monohydrate and streptozotocin were given at the dose rate of 50mg/kg body weight and 35mg/kg body weight, respectively. Calculated doses of alloxan were dissolved in 1ml sterile water and given as slow intravenous injection through ear followed by Streptozotocin in 1ml freshly prepared citrate buffer,

pH 4.6. Both the solutions were prepared just before use. At 9 hours after drug administration rabbits were administered 5ml of 25% dextroseintraperitoneally, and given 10% glucose in drinking water up to 24 hours. Fasting blood glucose levels were recorded regularly and rabbits with blood glucose levels above 200 mg/dl at day 7 were considered diabetic (Mir *et al.,* 2016). A total of 12 hyperglycemic rabbits and 12 placebo treated normoglycemic rabbits were used for the investigations up to 60 days.

Pathoanatomical studies

Rabbits, 2 each, from both alloxan-STZ treated and control groups were euthanized fortnightly up to day 60. Complete systematic necropsy (Rokitansky's method) was conducted. After recording of gross lesions, representative tissue samples from all the organs were collected in 10% formal saline.

The tissue samples were processed following routine paraffin embedding technique. Different grades of ethanol were used for dehydration and clearance was carried out by several changes in benzene. 4-5µm thickness sections were stained by Harris' haematoxylin and eosin method. Also, Alcian-Blue PAS (AB-PAS) staining was used for acid and neutral mucopolysaccharides demonstration (Luna, 1968).

Results and Discussion

Gross pathology

Rabbit dead or sacrificed revealed pale mucous membranes and congested viscera. Pancreas was soft, swollen and congested followed by thinning with reduced mass. Mesenteric vessels were consistently congested.

Liver was congested and darker having petechiae, ecchymosis and suffusions on visceral and parietal surfaces. Kidneys were darker, haemorrhagic and mottled, and studded with grayish white foci. Cut surface revealed both cortical and medullary congestion. Lung were voluminous and emphysematous and at later stages additionally showed congestion, haemorrhages and red hepatization (Fig. 1).

Histopathology

Pancreas

At day 15 pancreatic islets were variedly affected. While some islet cells appeared normal, others revealed degenerative and degranulative changes of beta-cells with increased eosinophilia. At other places islet cells had acquired cord like appearance (Fig 2a). Occasionally, islets revealed loss of beta cells resulting in mild to marked reduction in cellularity. The cells undergoing degeneration and necrosis revealed vacuolation and appeared fusiform in shape. Ghost islets, characterized by total cell loss, were, also, observed. Degenerative changes of acinar cells had resulted in severe distortion of acinar architecture. Vascular congestion was seen in the mesenteric attachment, interlobular septa and the parenchyma.

At day 30, most of the islets were smaller in size with beta-cells showing degeneration and degranulation. Necrosis of the cells had resulted in prominent islet disorganization. Marked hypocellularity of the islets was occasionally seen (Fig. 2b). Vascular congestion was mild and the acinar cells appeared normal.

At day 45, islet cells revealed degranulation and degeneration with increased eosinophilia. Necrosis of the beta-cell had caused mild to marked hypocellularity. Acinar cells continued to appear normal.

At day 60, islets were variably affected. Most of the islets were hypocellular due to degeneration and necrosis of beta-cells. The cells showed vacuolation followed by complete lysis (Fig. 2c). Occasionally, complete hyalinization of the cells was observed (Fig. 2d). Some islets appeared normocellular. Acinar were normal.

Liver

At day 15 marked congestion and haemorrhages were observed. Hepatosis included cellular swelling with hazy cytoplasm, and nuclear hypochromatism and rarefaction. Mononuclear cells infiltration was observed both in the portal areas and the parenchyma (Fig. 3a).

At day 30 hepatocellular degeneration, characterized by cellular swelling rounding of cells, vacuolar change and compression of sinusoids, was seen. Binucleated hepatocytes were observed. Focal hepatitis, characterized by mononuclear cell infiltration and kupffer cell hyperplasia, was observed (Fig. 3b) and was especially prominent in the periportal areas. Occasionally, cholangitis was associated with portal fibrosis.

At day 45, hepatosis continued but the sinusoids revealed marked dilatation (Fig. 3c). Portal triaditis was observed and was occassionally associated with vascular degeneration. Binucleated hepatocytes continued to exist.

At day 60 severe hepatocellular degeneration and necrosis were seen (Fig. 3d). Portal triaditis and congestion were prominent.

Kidney

At day 15 kidneys revealed severe cortical congestion and haemorrhages. Cellular degeneration of convoluted tubules was characterized by swelling with indistinct cell boundaries, rarefied nucleus and narrowing of tubluar lumens. Necrotic changes were more prominent in perivascular areas and were occasionally associated with damaged basement membrane and infiltration of mononuclear cells. Glomeruli were hypersegmented and congested (Fig. 4a). Mesangial cell hyperplasia and mild mononuclear cell infiltration were evident. Medullary congestion, haemorrhages and lower nephron nephrosis were seen. The collecting tubules revealed degeneration and necrosis of lining epithelium. Interstitial congestion and haemorrhages were prominent. At day 30, cortical tubular epithelium revealed marked degeneration with increased eosinophilia and granulation in cytoplasm, and necrosis but the basement membrane appeared intact. Interstitial fibroplasia was occasionally noted Glomeruli revealed hypertrophy causing reduced Bowman's space. Hypersegmentation, fragmentation of glomeruli associated with mesangial cell hyperplasia were frequently noted (Fig. 4b). Renal medulla revealed mild vascular congestion and degeneration of tubular epithelium. Severe peritubular fibrosis was noted.

At day 45, cortical tubular degeneration was denoted by cellular swelling resulting in narrowing of lumens. Frequently, tubular lining epithelial cells showed loss of nuclei and indistinct cell boundary. Nephrotic changes were more severe in subcapsular regions. Similarly, marked nephrosis was observed in the cortico-medullary junction along with focal haemorrhages and mild peritubular fibroplasia (Fig. 4c). Glomerular hypertrophy and hypersegmentation, and the vacuolation of podocytes was a prominent feature. Medulla revealed vascular congestion, focal haemorrhages and prominent lower nephron nephrosis.

At day 60 cortical tubules continued to show cellular swelling with increased eosinophilia and cytoplasmic granularity. Glomeruli persisted to reveal hypertrophy and hypersegmentation and vacuolation in the podocytes (Fig. 4d). Cytolysis was frequently observed along the periphery of glomeruli. Renal medullary tubules revealed vacuolar change and protenacious casts.

Brain

At day 15, Cerebral cortex revealed degeneration and necrosis of both granule as well as large and small pyramidal cells. The necrotic cells were shrunken with increased cytoplasmic basophilia, and nuclear pyknosis, karyorhexis and karyolysis. Mild satellatosis and neuronophagia were observed. Neuronal degeneration and necrosis, denoted by nuclear condensation and neuropil dilatation

associated with satellitosis and neuronophagia, were observed in caudoputamen, different areas of hippocampus including dentate gyrus and *Cornu Ammonis* especially pyramidal cells of CA4 region.

Extensive changes were observed in subiculum and brain stem. Medullary tracts revealed demyelination and gliosis (Fig. 5a). Vascular congestion was noted in meninges, brain cortex and choroid plexus. Cerebellum was congested and showed mild purkinje cell degeneration. Karyorrhexis was observed in cells of granule layer.

At day 30 changes were comparatively more severe. Cerebral cortex revealed widespread degeneration and necrosis of granule and pyramidal neurons associated with satellitosis and neuronophagia (Fig. 5b). Neuronal degeneration characterised by chromatolysis, nuclear pyknosis and dilation of perivascular space was observed in deeper cortex, caudoputamen, different areas of hippocampus including dentate gyrus, *Cornu Ammonis*, especially in the CA4 region and subiculum. Brain stem revealed neuronal degeneration and condensation along with dilated neuropil, demyelination, satellitosis, and neuronophagia. Demyelination was marked in medullary tracts. Meningeal congestion was marked. Cerebellum revealed focal degeneration and necrosis of purkinje cells.

At day 45, Cerebral cortex revealed degeneration and necrosis of granule and pyramidal neurons along with gliosis, satellitosis and neuronophagia (Fig. 5c). In basal regions of cerebrum and enorhinal cortex loss of neurons was marked and associated with severe demyelination giving it a vacuolar appearance. Similar changes were noted in caudoputamen, hippocampus proper, dentate gyrus, different areas of *Cornu Ammonis* especially CA4 and subiculum. Demyelination was markedly evident in medullary tracts. Degeneration and vacuolation of choroid epithelial cell was noted. However, congestion was comparatively less marked than at day15 or day30. Purkinje cell degeneration and necrosis was more marked than observed at previous days.

At day 60 cerebral cortex revealed neuronal degeneration and necrosis with chromatolysis, satellitosis and neuronophagia. At places marked necrosis with neuronophagic nodule formation was also observed (Fig. 5d). Degeneration and necrosis of neuronal and demyelination gave vacuolar appearance in caudoputamen. Similar changes were noted in different regions of hippocampus including dentate gyrus, *Cornu Ammonis*CA1, CA2, CA3 and CA4 regions and subiculum.

Medullary tracts revealed neuronal degeneration and necrosis with severe demyelination giving it a vacuolar appearance. Marked degeneration and vacuolation of choroid epithelium was noted.

Cerebellum revealed focal degeneration and necrosis of purkinje cells, and demyelination in the medullary region.

Lung

At days 15, lungs revealed marked vascular congestion, emphysema and mild alveolar haemorrhages (Fig. 6a). Changes were similar at day 30 but atelectasis was marked in the areas adjacent to emphysema, and peribronchial lymphoid hyperplasia was noted (Fig. 6b).

At day 45, besides emphysema and atelectasis, and haemorrhagic exudation into the bronchi and bronchioles were observed. Peribronchial lymphoid hyperplasia was marked (Fig. 6c). Occasionally pneumonic areas and hypertrophy of vascular walls were seen. At day 60 changes were similar but the pneumocytes revealed vacuolation (Fig. 6d). Macrophages were present within the alveoli.

Heart

At day 15, heart showed marked vascular congestion, degeneration of cardiomyocytes ands focal haemorrhages (Fig. 7a). Changes were progressive at days 30 and 45 and by day 60 necrosis of cardiomyocytes was more prominent (Fig. 7b).

Spleen

At day 15, spleen revealed congestion of sinusoids and depletion of lymphoid tissue which was marked at days 30, 45 and 60, (Fig. 8a). Reticular cells were either vacuolated or revealed increased cytoplasmic eosinophilia. Besides, at day 60 cytolysis of reticular cells and lymphoid cell apoptosis were prominent.

Mesenteric lymph node

At day 15 marked vascular congestion and haemorrhages were seen. Mild to moderate depletion of cortical lymphoid cells was noted. Medullary area, too, revealed marked lymphoid depletion and histiocytosis in the sinuses. Changes were similar at day 30 (Fig. 8b). At days 45 and 60 vascular congestion was less marked but the lymphoid depletion and histiocytic reaction was more conspicuous.

Adrenal gland

Up to day 30, adrenal gland showed mild to moderate congestion which had subsided by day 45. In cortex, cellular degeneration and necrotic changes were confined to zona glomerulosa and zona fasciculata (Fig. 8c). Medulla too showed marked degeneration and focal necrosis.

Testes

At day 15, testes appeared normal and by day 30, seminiferous tubules showed arrested spermatogenesis at the level of spermatogonia and primary spermatocytes in pachytene stage. Spermatogonial cells frequently appeared in multiple layers. Most of the tubules showed decreased number of spermatogonial cells. At day 45 changes were more marked and the lumen of seminiferous tubules contained homogenized cell remnants (Fig. 8d). At day 60, additionally vacuolation and apoptosis of spermatocytes was noted. Grossly palor of mucous membranes reflects anaemia. Generalized congestion and haemorrhages in different organs may be attributed to vascular changes associated with glucotoxicity or direct effects of the drug leading to oxidative stress (Doczi-Keresztesi *et al.,* 2012). Soft appearance of pancreas, and reduced mass at later stages may be attributed to beta-cytolytic effects leading to dumping of high insulin levels in the pancreas before being carried out in to circulation. Necrotic foci in kidneys and changes in lungs at advanced stage reflect glucolipotoxicity. Similar changes were noted in Alloxan diabetic rabbits as well as STZ treated normoglycemic rabbits

Histopathologically, Alloxan-STZ cocktail caused marked β-cell degeneration and necrosis in pancreas which may be attributed for observed hyperglycemia. The relatively normal appearing islets provide for residual insulin secretion favouring maintenance of animals without insulin therapy. Both Alloxan and STZ are β-cytotoxic drugs but result in partial cytolysis when administered at low doses (Aybar *et al.,* 2001; Szkudelski, 2001; Mir *et al.,* 2005; Elsner *et al.,* 2006; Mir and Darzi, 2009). During present study rabbit islets appeared to be partially resistant to STZ. However, the cocktail appeared to exert synergistic effect. Vacuolated fusiform cells and formation of cords has been observed in Alloxan diabetes (Mir *et al.,* 2005, 2016; Mir and Darzi, 2009). Persistence of degenerative changes may be attributed to hyperglycemic stress causing hypersecretion and exhaustion of β-cells (Liu *et al.,* 2000; Szkudelski, 2001; Poitout and Robertson, 2002; Rabuazzo *et al.,* 2003; Liu *et al.,* 2004; Slawson *et al.,* 2005; Pathak *et al.,* 2008; Arora *et al.,* 2009; Del-Prato, 2009).

More number of normal appearing islets were observed at later stage indicating regeneration (Finegood *et al.,* 1995; Pick *et al.,* 1998; Montanya 2000; Dor *et al.,* 2004; Bonner-Weir *et al.,* 2004; Grossman *et al.,* 2010), which correlated well with the glycemic status of rabbits. Exocrine changes observed have been attributed to direct effect of the drugs or heavy release of insulin from degranulating β-cells (Okabayashi *et al.,* 1988; Aughsteen and Kataoka, 1993; Meral *et al.,* 2001; Meral *et al.,* 2001; Burski *et al.,* 2004; Patel *et al.,* 2004 & 2006).

Fig.1 Alloxan-streptozotocin diabetic rabbits, a)Pancreas at day 15 appearing soft, oedematous and congested; b) Liver at day 60 revealing congestion and areas of suffusions; c) Kidney at day 60 revealing congestion and petechiae; d) Lungs at day 30 showing areas of congestion, suffusions and red hepatisation.

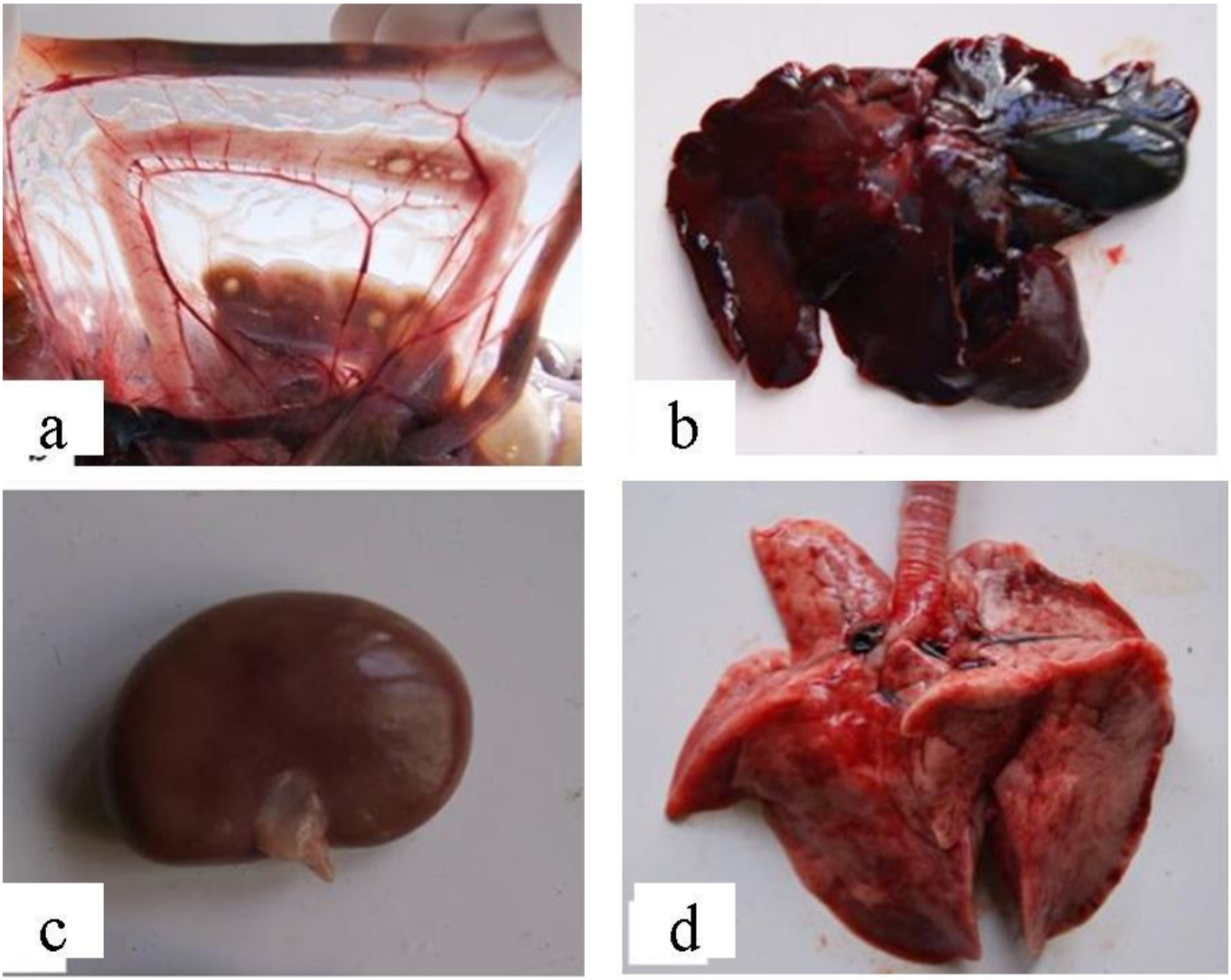

Fig.2 Section of pancreas a) day 15, Degenerated beta cells. H.E. x 400 (OZ x 4.0); b) day 30, Hypocellular islet with degeneratedand necrosed beta-cells. H.E. x 400 (OZ x 4.0); c) day 60, Moderately hypocellular islet. H.E. x 400 (OZ x 4.0); d) day 60, Hyalinization of islet cells. H.E. x 400 (OZ x 4.0);

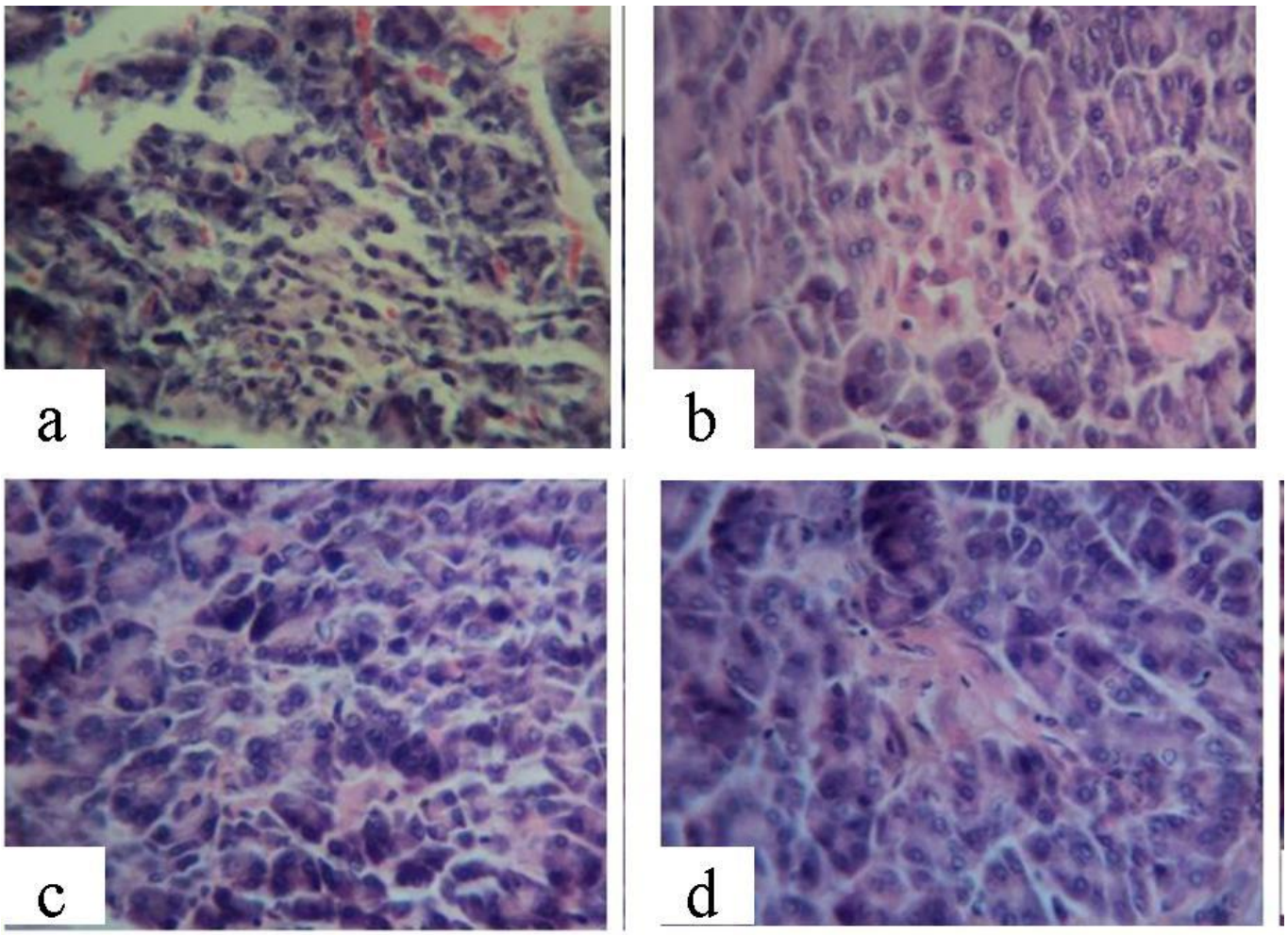

Fig.3 Section of livera) day 15, Vascular congestion, hepatocellular degeneration and mild infiltration of mononuclear cells in portal area. H.E. x 400 (OZ x 4.0); b) day 30, Mononuclear cell infiltration and mild fibroplasia around the central vein. H.E. x 400 (OZ x 4.0); c)Hepatocellular degeneration and dilatation of sinusoids. H.E. x 100 (OZ x 6.2); d) Hepatitis and presence of binucleated hepatocytes. H.E. x 100 (OZ x 6.2).

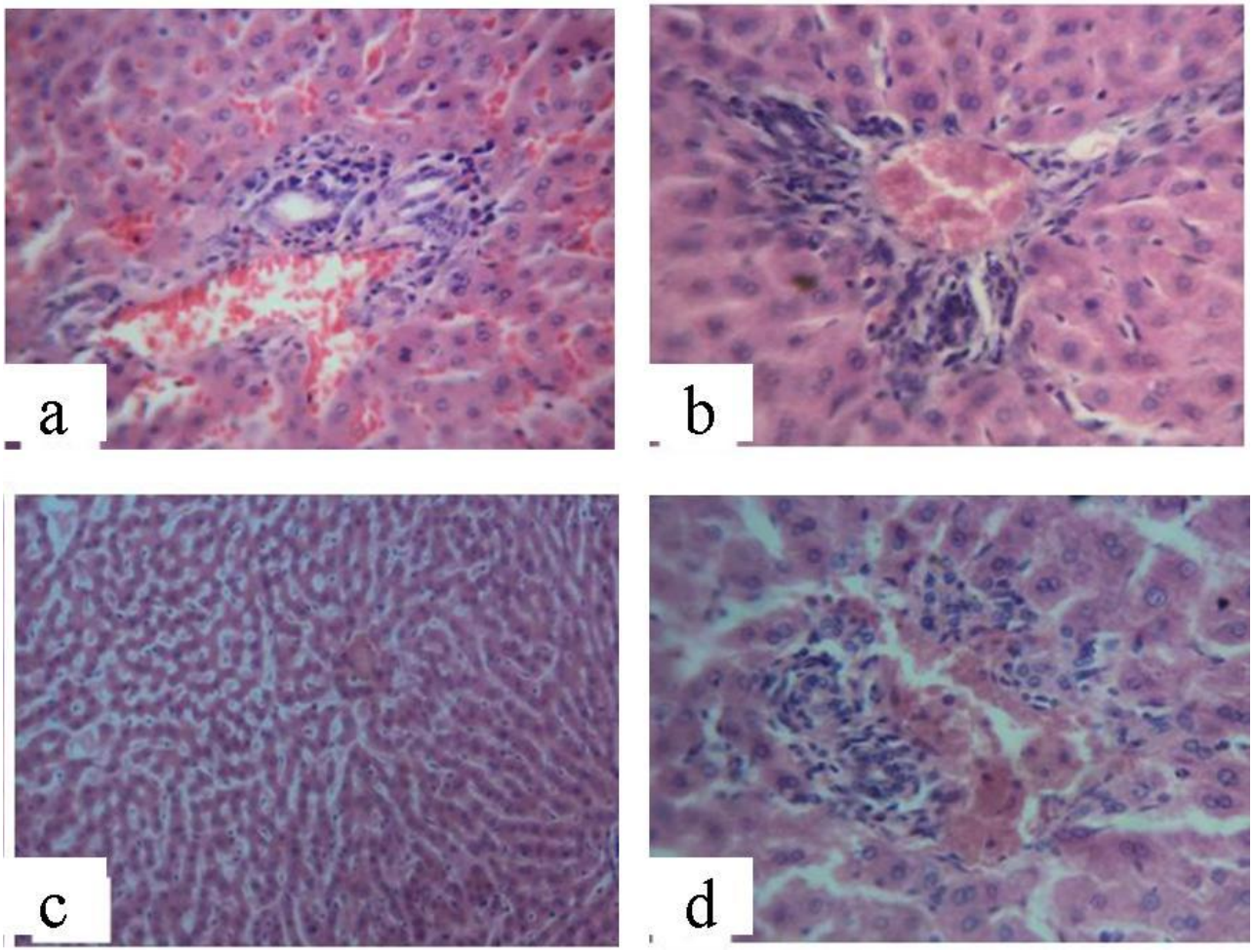

Fig.4 Section of Kidney a) day 15, Congestion and hypersegmentation of glomeruliand degeneration of tubular epithelium. H.E. x 400 (OZ x 4.0); b) day 30, Hypertrophy and segmentation of glomeruli, and mesangial cell hyperplasia. H.E. x 400 (OZ x 4.0);c) day 45, Mild peritubular fobroplasia and degenerative tubular epithelium. H.E. x 400 (OZ x 4.0); d) day 60, Glomerular hypersegmentationand cortical nephrosis. H.E. x 100 (OZ x 4.0); Insert : Higher magnification of Glomerulus showing vacuolation of podocytes. H.E. x 400 (OZ x 4.0).

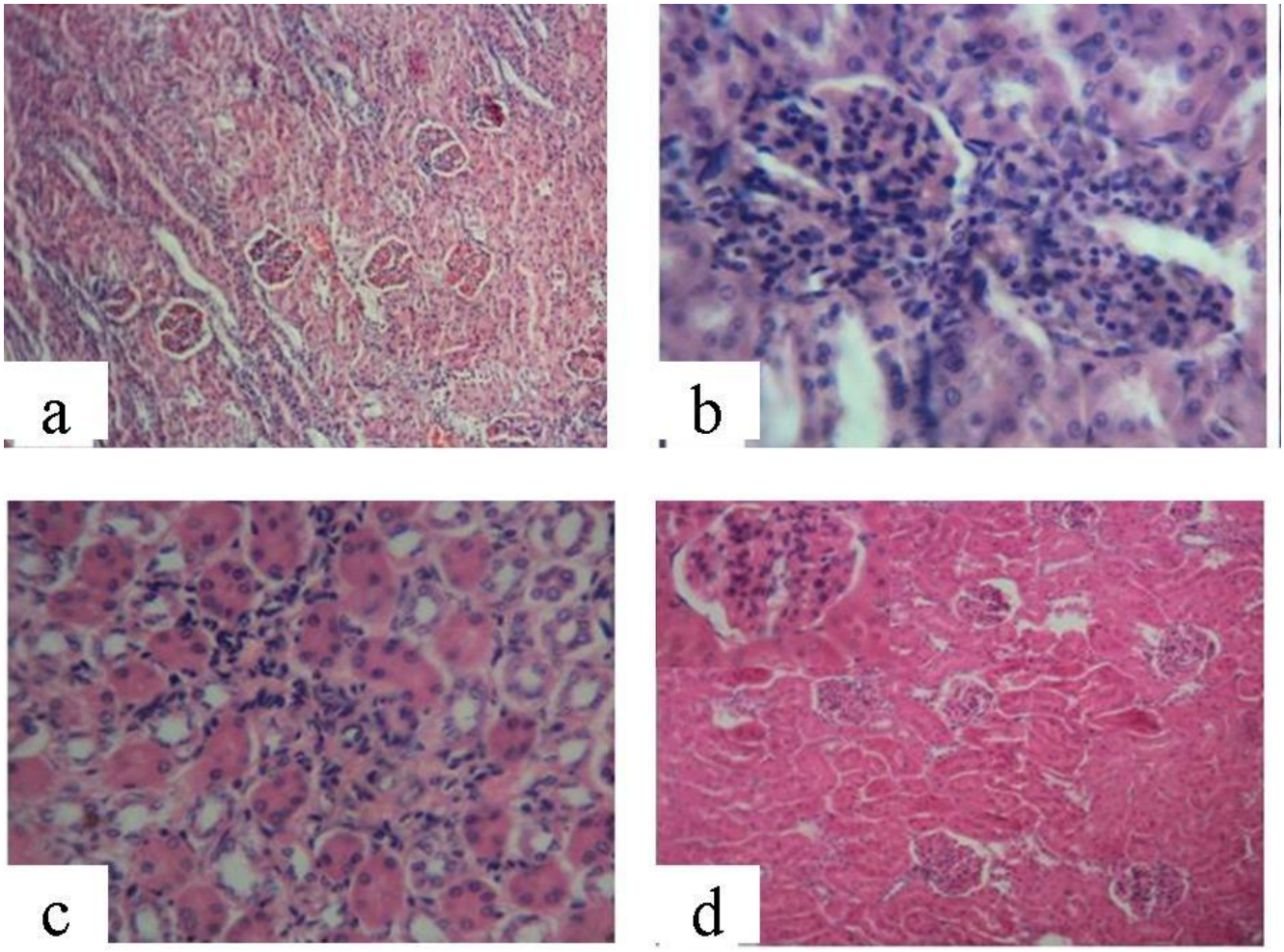

Fig.5 Section of brain a) day 15, Demyelination and gliosis in cerebrum. H.E. x 400 (OZ x 4.0); b) day 30, Widespread neuronal degeneration in outer cerebral cortex. H.E. x 100 (OZ x 4.0); c) day 45, Neuronal degeneration and necrosis in cerebral cortex. H.E. x 100 (OZ x 4.5);d) day 60, Neuronal degeneration, gliosis and dilatation of neuropil in cerebral cortex. H.E. x 100 (OZ x 4.0); Insert: Higher magnification of neuronophagic nodule. H.E. x 400 (OZ x 4.0);

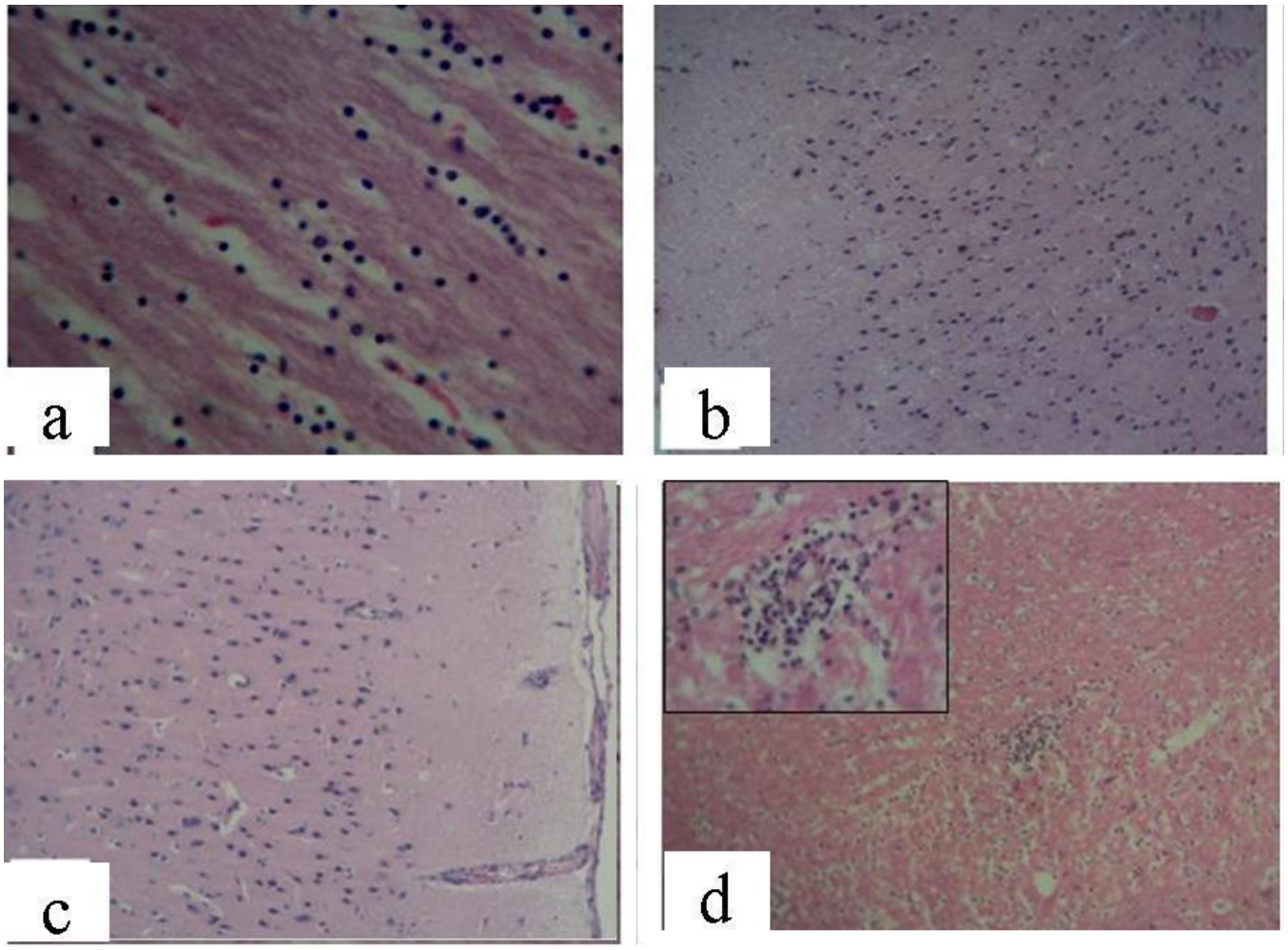

Fig.6 Section of lungs a) day 15, Vascular congestion and emphysema. H.E. x 100 (OZ x 3.0); b) day 30, Peribronchial lymphoid hyperplasia. H.E. x 100 (OZ x 4.0). c)Peribronchial lymphoid hyperplasia and haemorrhagic exudates in the bronchi. H.E. x 100 (OZ x 4.0) d) day 60, Vacuolation in the pneumocytes. H.E. x 100 (OZ x 4.0).

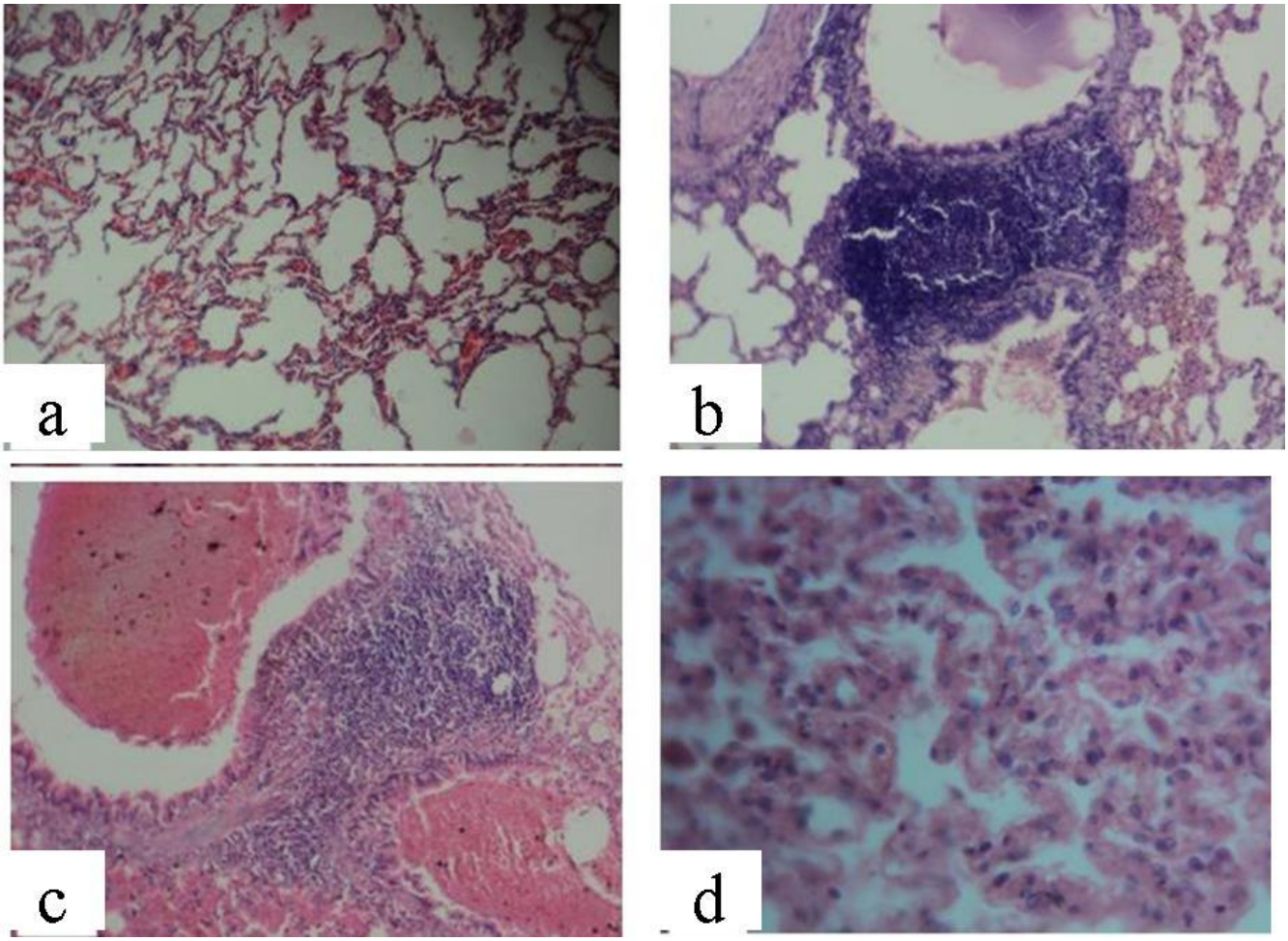

Fig.7 Section of heart a) day 15, Degeneration of cardiomyocytes and haemorrhage. H.E. x 400 (OZ x 4.0); b) day 60, Severe degeneration and necrosis of cardiomyocytes. H.E. x 400 (OZ x 4.5);

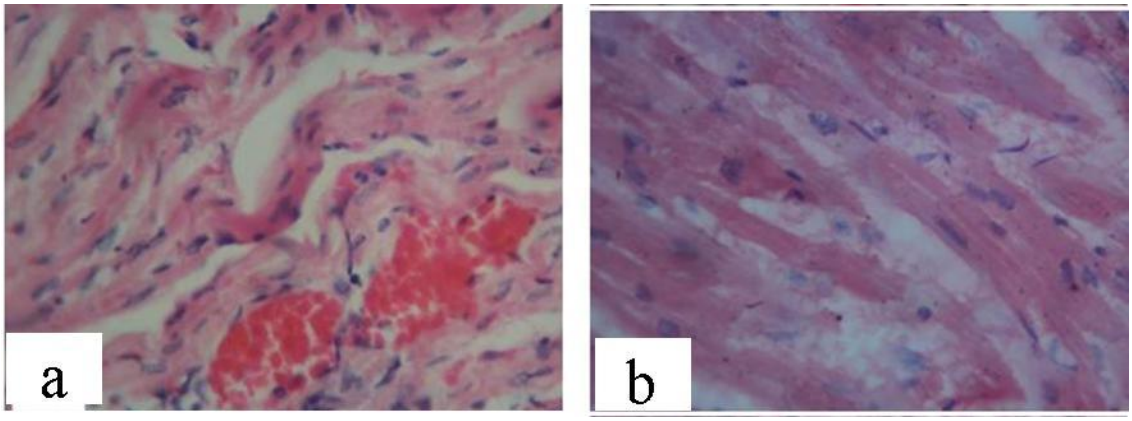

Fig.8 Section of a) spleen, day 30, revealing marked sinusoidal congestion and depletion of lymphoid tissue. H.E. x 100 (OZ x 4.0); b) mesenteric lymph node, day 30, Moderate lymphoid depletion. H.E. x 100 (OZ x 4.0); c) adrenal, day 45,Degeneration and necrotic changes in the cells of zona glomerulosa. H.E. x 400 (OZ x 4.0); d) testes, day 45, arrest of spermatogenesis. H.E. x 100 (OZ x 4.0);

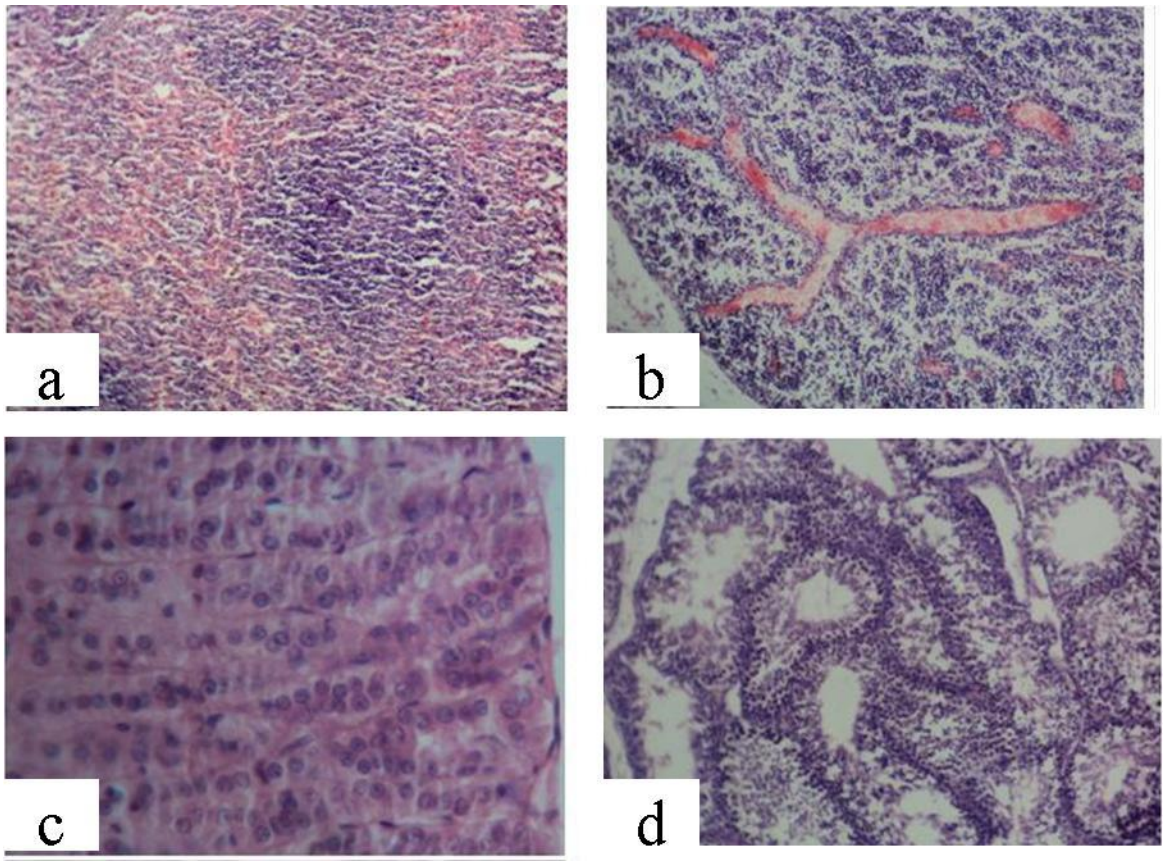

Liver revealed vascular congestion, progressive hepatosis, portal triaditis, and presence of binucleated hepatocytes. During later stage hepatocellular necrosis was seen. Similar changes have been reported by other workers in induced diabetic models (Sandhu *et al.,* 2000; Mir *et al.,* 2008b,d; Mir and Darzi, 2009; Zafar *et al.*, 2009b; Nahla and Refat, 2012). The changes have been attributed to glucolipotoxicity (Ohno *et al.*, 2000; Merzouk *et al.,* 2000; Poitout and Robertson, 2002; Schmeichel, *et al.,* 2003; El-Said *et al.,* 2010). The presence of binuclealed hepatocytes indicated regenerative process. Portaltriaditis has been reported in Alloxan and STZ induced diabetes and associated with either proinflammatory action of hyperglycemia and oxidative stress induced by the drugs (Zafar *et al.,* 2009b; Dasu and Jialal, 2011).

Kidneys revealed vascular congestion, focal haemorrhages, cortical tubular degeneration and necrosis, and lower nephron nephrosis. Glomeruli revealed congestion, hypersegmentation and mesangial cell hyperplasia. Later, peritubular fibroplasias, glomerular hypertrophy with vacuolation of podocytes and fragmentation and casts in collecting tubules were observed. Focal nephritis with mononuclear cell infiltration was seen. Varying degree of nephropathy has been reported in Alloxan (Mir *et al.,* 2005; Mir and Darzi, 2009) and STZ (Honjo *et al.,* 1986; Bansal *et al.,* 1994; Sandhu *et al.,* 2000; Zafar *et al.,* 2009a) diabetic animals.

The changes were milder than observed in Alloxan-diabetic rabbits. The nephrotic and nephritic changes have been attributed glucolipotoxicity (Rasch, 1984; Siu, *et al.*, 2006; Kramer *et al.,* 2009; Satriano *et al.,* 2010). Glomerular congestion and swelling, and mesangial cell hyperplasia has been recognized as characteristic feature of short-term diabetes, signifying proliferation of glomerular capillaries and increase in the volume of renal corpuscle (Bulut *et al.,* 2001). The oxidative stress associated with hypoxia and tubular epithelial damage may be incriminated for setting up of the proinflammatory response resulting in nephritis and peritubular fibroplasias (Tang *et al.,* 2003; Magri and Fava, 2009; Hirschberg and Wang, 2005; Ruster and Wolf, 2008; Vallon, 2011).

Brain revealed neuronal degeneration and necrosis with mild satellatosis and neuronophagia in cerebral cortex, caudoputamen, different areas of hippocampus including dentate gyrus and *Cornu Ammonis* especially pyramidal cells of CA4 region, subiculum and brain stem. Demyelination and gliosis was noted in medullary tracts. Vascular congestion was noted in meninges, brain cortex and choroid plexus. Cerebellum showed congested, mild purkinje cell degeneration and karyorrhexis in cells of granule layer. During later stage degeneration of choroid epithelium was noted. Although the changes were progressive, they were milder than both Alloxan diabetics and STZ treated rabbits. This may be attributed to lower dose of drugs reducing direct toxicity and development of milder hyperglycemia. Neuronophagic nodules and periependymal inflammation was not observed. Diabetes associated metabolic disturbances in brain has been reported to cause anatomical and functional disturbances, referred as diabetic encephalopathy, in humans as well as animal models (Mans *et al.,* 1988; Brands *et al.,* 2004; Allen *et al.,* 2004; Grünblatt *et al.,* 2007; Mir *et al.,* 2008c; Mir and Darzi, 2009; Hernández-Fonseca *et al.,* 2009; Plaschke *et al.,* 2010). The pathoanatomical alterations may be attributed to glucolipotoxicity (Edwards *et al.,* 2008; Ahamed, 2009; Arnal *et al.,* 2010; Shanmugam *et al.,* 2011; Alp *et al.,* 2012; Uzar *et al.,* 2012; Ceretta *et al.,* 2012).

Lungs revealed vascular congestion, haemorrhages, emphysema and atelectasis, and peribronchial lymphoid hyperplasia. At later stages focal pneumonic areas, hypertrophy of vascular walls, vacuolation of pneumocytes and presence of numerous alveolar macrophages were seen. Lungs have been recognized as target organs for diabetes (Schuyler *et al.,* 1976; Sahebjami and Denholm, 1988; Hsia and Raskin, 2007). Changes akin to present observations have been reported induced diabetic models (Sandhu *et al.,* 2000; Mir *et al.,*

2008a). Hyperglycemia induced ACh-mediated NO release and generation of ROS in endothelium have been demonstrates to play central role in diabetes associated pulmonary pathology (Nishikawa *et al.,* 2000b; Fouty, 2008) These ROS led to the activation of three potentially detrimental pathways in bovine aortic endothelial cells: activation of diacyl glycerol/protein kinase C, generation of AGE, and the generation of sorbitol due to activation of aldolase reductase, and pathological activation of these pathways has been implicated in the endothelial dysfunction associated with diabetes (Brownlee, 2005). Increased muscularization of pulmonary arteries of infants of diabetic mothers (Colpaert *et al.,* 1995) and specific type of nodular fibrosis of lung in diabetics (Farina *et al.,* 1995) have been described. Triglyceride deposition has been identified in the walls of pulmonary arteries of diabetic rats (Reinila *et al.,* 1977). Diabetes being a proinflammatory state might favour activation of resident macrophages. Popov and Simionescu (1997) observed that capillaries in lungs of diabetic hamsters contained adherent intravascular macrophages suggestive of an inflammatory process. The occurrence of pneumonic areas may be attributed to increased susceptibility to pulmonary infections (Moutschen *et al.,* 1992; Westphal *et al.,* 1994; Philips *et al.,* 2005).

Heart showed vascular congestion, focal haemorrhages and degeneration of cardiomyocytes. Also, necrosis of cardiomyocytes was more prominent at later stage. The changes may be attributed to persistent hyperglycemia and hyperlipidemia causing oxidative stress and hence vascular alterations. Similar changes have been reported in Alloxan and STZ induced diabetic models (Muruganandan *et al.,* 2002; Okoshi *et al.,* 2007; Mir *et al.,* 2008b,d; Mir and Darzi, 2009).

Spleen revealed congestion, haemorrhage, apoptosis of lymphoid cells, and vacuolation of reticular cells. Lymphoid depletion paralled leukocytopenia and may be attributed partly to observed apoptosis as well as proinflammatory effects of hyperglycemia favouring increased mobilization (Nichols *et al.,* 1981; Alexiewicz, 1997; Lenin *et al.,* 2012).Similar changes were observed in mesenteric lymph node. Besides, marked histiocytic reaction was noted. Glucolipotoxicity induced ROS have been found to cause activation of monocyte-macrophage cells in different tissues via NF-κB followed by cytokine release (Dasu and Jialal, 2011).

Adrenal gland revealed congestion, degeneration and necrosis in zona glomerulosa and zona fasciculate of cortex and in medulla. This may be attributed to hyperglycemia induced metabolic stress besides microvascular changes (Chan *et al.,* 2001; Sricharoenevj *et al.,* 2009).

Changes in testes were characteristic of arrested spermatogenesis, and degeneration and apoptosis of spermatocytes. Reproductive dysfunction have been associated with diabetes (Agbaje *et al.,* 2007; Amaral *et al.,* 2008), but the underlying mechanisms are poorly understood. Structural and functional alterations have been reported in STZ induced diabetic models (Hassan and Moneium, 2001; Ricci *et al.,* 2009). Oxidative stress induced activation of apoptotic pathway has been suggested as a mechanism for testicular alteration in diabetes (Koh, 2007; Zhao *et al.,* 2011).

The progressive and marked pathomorphological alterations suggest Alloxan-STZ diabetic rabbits shall be a good short term model for diabetes associated investigation when weighed appropriately against internal control. Further, the model needs to be evaluated at molecular level for deciphering the exact nature and mechanism of pathology.

References

Agbaje, I. M., Rogers, D. A., McVicar, C. M., McClure, N., Atkinson, A. B., Mallidis, C. and Lewis, S. E. 2007. Insulin dependent diabetes mellitus: implications for male reproductive function. *Human Reproduction*22:1871–1877.

Ahmed, N. 2009. Alloxan diabetes-induced oxidative stress and impairment of oxidative

defense system in rat brain: neuroprotective effects of *Cichorium intybus*. *International Journal of Diabetes and Metabolism*17:105-109.

Alexiewicz, J. M., Kumar, D., Smogorzewski, M. and Massry, S. G. 1997. Elevated cytosolic calcium and impaired proliferation of B lymphocytes in type II diabetes mellitus. *American Journal of Kidney Diseases*30:98–104.

Allen, K. V., Frier, B. M. and Strachan, M. W. J. 2004. The relationship between type 2 diabetes and cognitive dysfunction: longitudinal studies and their methodological limitations. *European Journal of Pharmacology*. 490(1–3):169–175.

Alp, H., Varol, S., Celik, M. M., Altas, M., Evliyaoglu, O., Tokgoz, O., Tanrıverdi, M. H. and Uzar, E. 2012. Protective effects of beta glucan and gliclazide on brain tissue and sciatic nerve of diabetic rats induced by streptozosin. *Experimental Diabetes Research*2012:230342.

Amaral, S., Oliveira, P. J. and Ramalho-Santos, J. 2008. Diabetes and the impairment of reproductive function: possible role of mitochondria and reactive oxygen species. *Current Diabetes Reviews*4:46–54.

Arnal, E., Miranda, M., Barcia, J., Bosch-Morell, F. and Romero, F. J. 2010. Lutein and docosahexaenoic acid prevent cortex lipid peroxidation in streptozotocin-induced diabetic rat cerebral cortex. *Neuroscience*166(1):271–278.

Arora, S., Ojha, S. K. and Vohora, D. 2009. Characterisation of streptozotocin induced diabetes mellitus in swiss albino mice. *Global Journal of Pharmacology*3 (2):81-84.

Aughsteen, A. A. and Kataoka, K. 1993. Morphometric studies on the juxta-insular and tele-insular acinar cells of the pancreas in normal and streptozotocin-induced diabetic rats. *J. Electron. Microsc. (Tokyo)*42:79–87.

Aybar, M. J., Sanchej Riera An., Grau, A. and Sanchez, S. S. 2001. Low dose of STZ produced an incomplete destruction of pancreatic β-cells in rats. *Journal of Ethnopharmacology*27: 243-247.

Bansal, B. K., Mohan, R., Bansal, N., Pawar, H. S. and Nauriyal, D. C. 1994. Alloxan diabetes in dogs: clinical and pathoanatomical observations. *Indian Journal of Veterinary Pathology*18(2): 138-141.

Bonner-Weir, S., Toschi, E., Inada, A., Reitz, P., Fonseca, S. Y., Aye, T. and Sharma, A. 2004. The pancreatic ductal epithelium serves as a potential pool of progenitor cells. *Pediatric Diabetes*5(Suppl):216–222.

Brands, A. M., Kessels, R. P., de Haan, E. H., Kappelle, L. J. and Biessels, G. J. 2004. Cerebral dysfunction in type I diabetes: effects of insulin, vascular risk factors and blood-glucose levels. *European Journal of Pharmacology*, 490(1–3):159–168.

Brownlee, M. 2005. The pathobiology of diabetic complications: a unifying mechanism. *Diabetes*54:1615–1625.

Bulut, H. E., Onarlioglu, B., Kaloglu, C., Ozdemir, O. and Ayan, S. 2001. Effects of experimental diabetes and insulin treatment on rabbit renal morphology: a quantitative and qualitative study. *Turkish Journal of Medical Sciences*31:209-216.

Burski, K., Ueland, T. and Maciejewski, R. 2004. Serum amylase activity disorders in the course of experimental diabetes in rabbits. *Veterinarni Medicina*49:197-200.

Ceretta, L. B., Réus, G. Z., Abelaira, H. M., Ribeiro, K. F., Zappellini, G., Felisbino, F. F., Steckert, A. V., Dal-Pizzol, F. and Quevedo, J. 2012. Increased oxidative stress and imbalance in antioxidant enzymes in the brains of Alloxan-induced diabetic rats. *Experimental Diabetes Research* 2009 ID 302682: 8 pages.

Chan, O., Chan, S., Inouye, K., Vranic, M. and Matthews, S. G. 2001.Molecular regulation of the hypothalamo-pituitary-adrenal axis in streptozotocin-induced diabetes: effects of insulin treatment. *Endocrinology* 142:4872–4879.

Colpaert, C., Hogan, J., Stark, A. R., Genest, D. R., Roberts, D., Reid, L. and Kozakewich, H. 1995 Increased muscularization of small pulmonary arteries in preterm infants of diabetic mothers: a morphometric study in noninflated, noninjected, routinely fixed lungs. *Pediatric Pathology and Laboratory Medicine*15:689–705.

Dasu, M. R. and Jialal, I. 2011. Free fatty acids in the presence of high glucose amplify monocyte inflammation via Toll-like receptors. *American Journal of Physiology – Endocrinology and Metabolism*300(1):E145-E154.

Del-Prato, S. 2009. Role of glucotoxicity and lipotoxicity in the pathophysiology of Type 2 diabetes mellitus and emerging treatment strategies. *Diabetic Medicine*26(12):1185-92.

Doczi-Keresztesi, Z., Jung, J., Kiss, I., Mezei, T., Szabo, L. and Ember, I. 2012. Retinal and renal vascular permeability changes caused by stem cell stimulation in alloxan-induced diabetic rats, measured by extravasation of fluorescein. *In Vivo* 26(3):427-35.

Dor, Y., Brown, J., Martinez, O. I. and Melton, D. A. 2004. Adult pancreatic β cells are formed by self-duplication rather than stem cell differentiation. *Nature*429:41-46.

Edwards, J. L., Vincent, A. M., Cheng, H. T. and Feldman, E. L. 2008. Diabetic neuropathy: Mechanisms to management. *Pharmacology and Therapeutics*120(1):1–34.

El-Said, E. E., El-Sayed, G. R. and Tantawy, E. 2010. Effect of camel milk on oxidative stress in experimentally induced diabetic rabbits. *Veterinary Research Forum*1(1):30-43.

Elsner, M., Gurgul-Convey, E. and Lenzen, S. 2006. Relative importance of cellular uptake and reactive oxygen species for the toxicity of alloxan and dialuric acid to insulin-producing cells. *Free Radical Biology and Medicine* 41:825–834.

Ettaro, L., Songer, T. J., Zhang, P., Engelgau, M. M. 2004. Cost-of-illness studies in diabetes mellitus. *Pharmacoeconomics*22:149-164.

Etuk, E. U. 2010. Animal models for studying diabetes mellitus. *Agriculture and Biology Journal of North America*1(2):130-134.

Farina, J., Furio, V., Fernandez-Acenero, M. J., Muzas, M. A. 1995. Nodular fibrosis of the lung in diabetes mellitus. *Virchows Archiv*427:61–63.

Finegood, D. T., Scaglia, L. and Bonner-Weir, S. 1995. Dynamics of beta-cell mass in the growing rat pancreas. Estimation with a simple mathematical model. *Diabetes*44:249–256.

Fouty, B. 2008. Diabetes and the pulmonary circulation. *American Journal of Physiology*-Lung *Physiology* 295(5):L725-L726.

Grossman, E. J., Lee, D. D., Tao, J., Wilson, R. A., Park, S. Y., Bell, G. I. and Chong, A. S. 2010. Glycemic control promotes pancreatic beta-cell regeneration in streptozotocin-induced diabetic mice. *PLoS ONE*5(1):e8749.

Grünblatt, E., Salkovic-Petrisic, M., Osmanovic, J., Riederer, P. and Hoyer, S. 2007. Brain insulin system dysfunction in streptozotocin intracerebroventricularly treated rats generates hyperphosphorylated tau protein. *Journal of Neurochemistry*101(3):757-70.

Hassan, G. M. A. and Moneium, T. A. 2001.Structural changes in the testes of streptozotocin-induced diabetic rats. *Suez Canal University Medical Journal*4(1):17-25.

Hernandez-Fonseca, J. P., Rincón, J., Pedreañez, A., Viera, N., Arcaya, J. L., Carrizo, E. and Mosquera, J. 2009. Structural and ultrastructural analysis of cerebral cortex, cerebellum, and hypothalamus from diabetic rats. *Experimental Diabetes Research* 2009(ID329632): pages 12. doi: 10.1155/2009/329632

Hirschberg, R. and Wang, S. 2005. Proteinuria and growth factors in the development of tubulointerstitial injury and scarring in kidney disease. *Current Opinion in Nephrology and Hypertension* 14:43–52.

Honjo, K. Doi, K., Doi, C. and Mitsuoka, T. 1986. Histopathology of streptozotocin-induced diabetic DBA/2N and CD-1 mice. *Laboratory animals*20:298-303.

Hsia, C. C. and Raskin, P. 2007. Lung function changes related to diabetes mellitus. *Diabetes Technology and Therapeutics*9(1):S73-82.

King, A. J. F. 2012. The use of animal models in diabetes research. *British Journal of Pharmacology*, 166: 877-894

Koh, P. O. 2007. Streptozotocin-induced diabetes increases the interaction of Bad/Bcl-XL and decreases the binding of pBad/14-3-3 in rat testis. *Life Science*81:1079–1084.

Kottaisamy, C. P. D., Raj, D. S., Kumar, V. P. and Sankaran, U. 2021. Experimental animal models for diabetes and its related complications—a review. *Laboratory Animal Research*, 37:23; https://doi.org/10.1186/s42826-021-00101-4

Kramer, J., Moeller, E. L., Hachey, A., Mansfield, K. G. and Wachtman, L. M. 2009. Differential expression of GLUT2 in pancreatic islets and kidneys of New and Old World nonhuman primates. *American Journal of Physiology- Regulatory. Integrative and Comparative Physiology*296(3): R786–R793.

Lenin, R., Maria, M. S., Agrawal, M., Balasubramanyam, J., Mohan, V. and Balasubramanyam, M. 2012. Amelioration of Glucolipotoxicity-Induced Endoplasmic Reticulum Stress by a "Chemical Chaperone" in Human THP-1 Monocytes. *Experimental Diabetes Research* 2012(Article ID 356487):10 pages.

Liu, J. P., Zhang, M., Wang, W. Y. and Grimsgaard, S. 2004. Chinese herbal medicines for type-2 diabetes mellitus. *Cochrane Database of Systematic Reviews*3:3642.

Liu, K., Paterson, A. J., Chin, E. and Kudlow, J. E. 2000. Glucose stimulates protein modification by O-linked GlcNAc in pancreatic β cells: linkage of O-linked GlcNAc to β cell death. *Proceedings of National Academy of Science USA*97:2820–2825.

Luna L. G., 1968. *Manual of Histologic Staining Methods of the Armed Forces Institute of Pathology*, (3rd Edn.), McGraw-Hill Book Company, New York.

Magri, C. J. and Fava, S. 2009. The role of tubular injury in diabetic nephropathy. *European Journal of Internal Medicine* 20: 551–555.

Mans, A. M., Dejoseph, M. R., Davis, D. W. and Hawkins, R. A. 1988. Brain energy metabolism in streptozotocin-diabetes. *Biochemical Journal* 249:57-62.

Meral, I., Yener, Z., Kahraman, T. and Mert, N. 2001. Effect of Nigella sativa on glucose concentration, lipid peroxidation, anti-oxidant defence system and liver damage in experimentally-induced diabetic rabbits. *Journal of veterinary medicine. A, physiology, pathology, clinical medicine*48:593–599.

Merzouk, H., Madani, S., Chabane, S. D., Prost, J., Bouchenak, M. and Belleville, J. 2000. Time course of changes in serum glucose, insulin, lipids and tissue lipase activities in macrosomic offspring of rats with Streptozotocin induced diabetes. *Clinical Science*98(1):21-30.

Mir, M. S., Darzi, M. M., Baba, O. K., Khan, H. M., Kamil, S. A., Sofi, A. H. and Wani, S. A. 2015. Streptozotocin induced acute clinical effects in rabbits (*Oryctolagus cuniculas*). *Iranian Journal of Pathology*, 10(3):206-213.

Mir, M. S., Darzi, M. M., Baba, O. K., Shah, A. A., Qureshi, S. and Khan, H. M., 2016. Comparative evaluation of diabetogenic potentials of alloxan, streptozotocin and their cocktail in rabbits(*Oryctolagus cuniculas*). *Applied Biological Research*, 18: 61-65; DOI: 10.5958/0974-4517.2016.00009.4

Mir, S. H. and Darzi, M. M. 2009. Histopathological abnormalities of prolonged alloxan-induced diabetes mellitus in rabbits. *International journal of Experimental Pathology*90:66-73.

Mir, S. H., Baqui, A., Bhagat, R. C., Darzi, M. M.

and Mir, M. S. 2008a. Histopathological study of lung in prolonged Alloxan-induced diabetes mellitus in rabbits. *Indian Journal of Applied and Pure Biochemistry*23(1):147-151.

Mir, S. H., Baqui, A., Bhagat, R. C., Darzi, M. M. and Shah, A. W. 2008b. Biochemical and histomorphological study of streptozotocin-induced diabetes mellitus in rabbits. *Pakistan Journal of Nutrition*7(2):359-364.

Mir, S. H., Baqui, A., Bhagat, R. C., Darzi, M. M., Mir, M. S. and Shah, A. W. 2008c. Study on Induced Experimental Diabetes in Relation to Rabbit Brain. *Asian Journal of. Experimental Science*22(1):49-54.

Mir, S. H., Baqui, A., Darzi, M. M. and Mir, M. S. 2005. Pathoanatomy of experimental diabetes in rabbits (*Oryctolagus cuniculus*). *Oriental Science,*10(2):67-70.

Mir, S. H., Darzi, M. M., Ahmad, F., Chishti, M. Z. and Mir, M. S. 2008d. The influence of Glimepiride on the biochemical and histomorphological features of streptozotocin – induced diabetic rabbits. *Pakistan Journal of Nutrition*7(3):404-407.

Montanya, E., Nacher, V., Biarnes, M. and Soler, J. 2000. Linear correlation between beta-cell mass and body weight throughout the lifespan in Lewis rats: role of beta-cell hyperplasia and hypertrophy. *Diabetes*49:341–1346.

Moutschen, M. P., Scheen, A. J., Lefebre, P. J. 1992. Impaired immune responses in diabetes mellitus: analysis of the factors and mechanisms involved. Relevance to the increased susceptibility of diabetic patients to specific infections. *Diabetes and Metabolism*18:187–201.

Muruganandan, S., Gupta, S., Kataria, M., Lal, J. and Gupta, P. K. 2002. Mangiferin protects the streptozotocin-induced oxidative damage to cardiac and renal tissues in rats. *Toxicology*176(3):165-173.

Nahla, A. G. and Refat, A. 2012. Efficacy of N. sativa oil and Glimepiride on the histopathological changes of streptozotocin-induced diabetic rats. *Journal of American Science*8(3):22-33.

Nichols, W. K., Vann, L. L and Spellman, J. B. 1981. Streptozotocin effects on T lymphocytes and bone marrow cells. *Clinical and Experimental Immunology*46(3):627–632.

Nishikawa, T., Edelstein, D., Du, X. L., Yamagishi, S., Matsumura, T., Kaneda, Y., Yorek, M. A., Beebe, D., Oates, P. J., Hammes, H. P., Giardino, I. and Brownlee, M. 2000b. Normalizing mitochondrial superoxide production blocks three pathways of hyperglycaemic damage. *Nature* 404:787–790.

Noshahr, Z. S., Salmani, H., Rad, A. K., and Sahebkar, A. 2020. Animal models of diabetes-associated renal injury. *Journal of Diabetes Research, 9416419: 16 pages*

Ohno, T., Horio, F., Tanaka, S., Terada, M., Namikawa, T. and Kitch, J. (2000). Fatty liver and hyperlipidemia in IDDM (insulin dependent diabetes mellitus) of Streptozotocin treated shrews. *Life Science*66(2):125-131.

Okabayashi, Y., Otsuki, M., Ohki, A., Suehiro, I. and Baba, S. 1988. Effect of diabetes mellitus on pancreatic exocrine secretion from isolated perfused pancreas in rats. *Digestive Diseases and Sciences*33:711–717.

Okoshi, K., Guimarães, J. F. C., Di Muzio, B. P., Fernandes, A. A. H. and Okoshi, M. P. 2007. Miocardiopatia diabetic (Diabetic cardiomyopathy). *Arquivos Brasileiros de Endocrinologia and Metabologia* 51(2):160-167.

Patel, R., Shervington, A., Pariente, J. A., Martinez-Burgos, M. A., Salido, G. M., Adeghate, E. and Singh, J. 2006. Mechanism of exocrine pancreatic insufficiency in streptozotocin-induced type 1 diabetes mellitus. *Annals of the New York Academy of Sciences*1084:71–88.

Patel, R., Yago, M. D., Mañas, M., Victoria, E. M., Shervington, A. and Singh, J. 2004. Mechanism of exocrine pancreatic

insufficiency in streptozotocin-induced diabetes mellitus in rat: effect of cholecystokinin-octapeptide. *Molecular and Cellular Biochemistry*261(1-2):83-89.

Pathak, S., Dorfmueller, H. C., Borodkin, V. S. and van Aalten, D. M. F. 2008. Chemical dissection of the link between streptozotocin, O-GlcNAc, and pancreatic cell death. *Chemical Biology*15(8):799–807.

Philips, B., Redman, J., Brennan, A., Wood, D., Holliman, R., Baines, D. and Baker, E. 2005. Glucose in bronchial aspirates increases the risk of respiratory MRSA in intubated patients. *Thorax*60(9):761–764.

Pick, A., Clark, J., Kubstrup, C., Levisetti, M., Pugh, W., Bonner-Weir, S. and Polonsky, K. S. 1998. Role of apoptosis in failure of beta-cell mass compensation for insulin resistance and beta-cell defects in the male Zucker diabetic fatty rat. *Diabetes*47:358–364.

Plaschke, K., Kopitz, J., Siegelin, M., Schliebs, R., Salkovic-Petrisic, M., Riederer, P. and Hoyer, S. 2010. Insulin-resistant brain state after intracerebroventricular streptozotocin injection exacerbates Alzheimer-like changes in Tg2576 AbetaPP-overexpressing mice. *Journal of Alzheimer's Disease*19(2):691-704.

Poitout, V. and Robertson, R. P. 2002. Minireview: Secondary β-cell failure in Type 2 diabetes—A convergence of glucotoxicity and lipotoxicity. *Endocrinology*143:339 – 342..

Popov, D. and Simionescu, M. 1997. Alterations of lung structure in experimental diabetes, and diabetes associated with hyperlipidaemia in hamsters. *European Respiratory Journal*10:1850–1858.

Rabuazzo, A. M., Piro, S., Anello, M., Patanè, G. and Purrello, F. 2003. Glucotoxicity and lipotoxicity in the beta cell. *International Congress Series*1253:115–121.

Rasch, R. 1984. Tubular lesions in streptozotocin diabetic rats. *Diabetologia*27:32-37.

Reinila, A., Koivisto, V. A. and Akerblom, H. K. 1977. Lipids in the pulmonary artery and the lungs of severely diabetic rats. A histochemical and chemical study. *Diabetologia*13:305–310.

Ricci, G., Catizone, A., Esposito, R., Pisanti, F. A., Vietri, M. T. and Galdieri, M. 2009. Diabetic rat testes: morphological and functional alterations. *Andrologia*41(6):361-368.

Ruster, C. and Wolf, G. 2008. The role of chemokines and chemokine receptors in diabetic nephropathy. *Frontiers in Bioscience*13:944–955.

Sahebjami, H. and Denholm, D. 1988. Effects of streptozotocin-induced diabetes on lung mechanics and biochemistry in rats.*Journal of Applied Physiology*64(1):147-153.

Sandhu, K., Randhawa, S. S. and Brar, R. S. 2000. Clinical and pathological changes in alloxan induced diabetes mellitus alone and in combination with ethylene glycol induced nephropathy in dogs. *Indian Journal of Veterinary Pathology*24:12–15.

Satriano, J., Mansoury, H., Deng, A., Sharma, K., Vallon, V., Blantz, R. C. and Thomson, S. C. 2010. Transition of kidney tubule cells to a senescent phenotype in early experimental diabetes. *American Journal of Physiology - Cell Physiology* 299:C374–C380.

Schmeichel, A. M., Schmelzer, J. D. and Low, P. A. 2003. Oxidative injury and apoptosis of dorsal root ganglion neurons in chronic experimental diabetic neuropathy. *Diabetes*52(1):165-171.

Schuyler, M., Niewoehner, D. Inkley, S. and Kohn, R. 1976. Abnormal lung elasticity in juvenile diabetes mellitus. *The American review of respiratory disease*113:37–41.

Shanmugam, K. R., Mallikarjuna, K., Kesireddy, N. and Sathyavelu Reddy, K. 2011. Neuroprotective effect of ginger on anti-oxidant enzymes in streptozotocin-induced diabetic rats. *Food and Chemical Toxicology*49(4):893–897.

Siu, B., Saha, J., Smoyer, W. E., Sullivan, K. A. and Brosius, F. C. 2006. Reduction in podocyte density as a pathologic feature in early diabetic nephropathy in rodents: prevention

by lipoic acid treatment. *BMC Nephrology*7:6.

Slawson, C., Zachara, N. E., Vosseller, K., Cheung, W. D., Lane, M. D. and Hart, G. W. 2005. Perturbations in O-linked β-N-acetylglucosamine protein modification cause severe defects in mitotic progression and cytokinesis. *Journal of Biological Chemistry*280:32944–32956.

Sricharoenvej, S., Boonprasop, S., Lanlua, P., Piyawinijwong, S. and Niyomchan, A. 2009. Morphological and microvascular changes of the adrenal glands in streptozotocin-induced long-term diabetic rats. *Italian Journal of Anatomy and Embryology* 114(1):1-10.

Srinivasan, K. and Ramarao, P. 2007. Animal models in type 2 diabetes research: An overview. *Indian Journal of Medical Research* 125:451-472.

Szkudelski, T. 2001. The mechanism of alloxan and streptozotocin action in β-cells of the rat pancreas. *Physiological Research* 50:536-546.

Tang, S., Leung, J. C., Abe, K., Chan, K. W., Chan, L. Y., Chan, T. M. and Lai, K. N. 2003. Albumin stimulates interleukin-8 expression in proximal tubular epithelial cells in vitro and in vivo. *The Journal of Clinical Investigation*111:515–527.

Thatte, U. 2009. Still in search of herbal medicine. *Indian Journal of Pharmacology*41:1-3.

Uzar, E., Alp, H., Cevik, M.U., Fırat, U., Evliyaoglu, O., Tufek, A. and Altun, Y. 2012. Ellagic acid attenuates oxidative stress on brain and sciatic nerve and improves histopathology of brain in streptozotocin-induced diabetic rats. *Neurological Sciences*33(3):567-74.

Vallon, V. 2011. The proximal tubule in the pathophysiology of the diabetic kidney. American Journal of Physiology - Regulatory, Integrative and Comparative Physiology 300:R1009–R1022.

Westphal, S. A. and Sarosi, G. A. 1994. Diabetic ketoacidosis associated with pulmonary coccidioidomycosis. *Clinical Infectious Diseases* 18:974–978.

Zafar, M., Naqvi, S. N., Ahmed, M. and Kaimkhani, Z. A. 2009a. Altered kidney morphology and enzymes in streptozotocin-induced diabetic rats. *International Journal of Morphology*27(3):783-790.

Zafar, M., Naqvi, S. N. H., Ahmed, M. and Kaimkhani, Z. A. 2009b. Altered liver morphology and enzymes in streptozotocin induced diabetic rats. *International Journal of Morphology*27(3):719-725.

Zhao, Y., Tan, Y., Dai, J., Li, B., Guo, L., Cui, J., Wang, G., Shi, X., Zhang, X., Mellen, N., Li, W. and Cai, L. 2011. Exacerbation of diabetes-induced testicular apoptosis by zinc deficiency is most likely associated with oxidative stress, p38 MAPK activation, and p53 activation in mice. *Toxicology Letters*200:100–106.

How to cite this article:

Masood Saleem Mir, Reashma Roshan, Omer Khalil Baba, Majid Shafi, Showkeen Muzamil Bashir and Imtiyaz Wani. 2022. Pathological Characterization of the Low Doses Alloxan-STZ Diabetic Rabbit Model. *Int.J.Curr.Microbiol.App.Sci.* 11(02): 67-87. doi: https://doi.org/10.20546/ijcmas.2022.1102.010